



## RECTANGULAR GUSSET PLATE BEHAVIOUR IN COLD-FORMED I-TYPE STEEL CONNECTIONS

Ž. BUČMYS<sup>1</sup>, A. DANIŪNAS<sup>2</sup>

Cold-formed structure connections utilizing gusset plates are usually semi-rigid. This paper investigates the behaviours of rectangular gusset plates in cold-formed connections of elements whose columns and beams are made with lipped back-to-back C-sections. Methods of calculating strength and stiffness are necessary for such semi-rigid joints. The main task of this paper is to determine a method capable of calculating these characteristics. The proposed analytical method could then be easily adapted to the component method that is described in part 1993-1-8 of the Eurocode. This method allows us to calculate both the strength and stiffness of rectangular gusset plates, assuming that the joint deforms only in plane. This method of design moment resistance calculation was presented taking into account that an entire cross-section shall reach its yield stress. A technique of stiffness calculation was presented investigating the sum of deformations acquired at the bending moment and from shear forces which are transmitted from each beam bolt group.

Calculation results according to the suggested method show good agreement of laboratory experimental results of specimens with numerical simulations. Two specimens of beam-to-column connections were tested in the laboratory. Lateral supports were used on the specimens to prevent lateral displacements in order to better investigate the behaviour of the rectangular gusset plate in plane. Experiments were simulated by modelling rectangular gusset plates using standard finite element software ANSYS Workbench 14.0. Three-dimensional solid elements were used for modelling and both geometric and material nonlinear analysis was performed.

*Keywords:* cold-formed steel connections, semi-rigid connections, strength, stiffness

---

<sup>1</sup> MSc. Eng., Vilnius Gediminas Technical University, Faculty of Civil Engineering, Saulėtekio al. 11, LT-10223 Vilnius, Lithuania, e-mail: zilvinas.bucmys@vgtu.lt

<sup>2</sup> Prof., Dr. Eng., Vilnius Gediminas Technical University, Faculty of Civil Engineering, Saulėtekio al. 11, LT-10223 Vilnius, Lithuania, e-mail: alfonsas.daniunas@vgtu.lt

## 1. INTRODUCTION

Cold-formed thin-walled sections are widely used as bearing structures. In most cases, thin-walled sections are used as purlins, steel trusses, and for lightweight portal frames. There is a wide variety of cold-formed sections (such as Z-sections, C-sections, sigma-sections, omega-sections, etc.). The connections of such structures should be simple, fast, and easily installed. Cold-formed sections can be connected using gusset plates and bolts, or directly using bolts; [1], screws [2], mechanical clinching [3], and welds. One of the easiest ways to make beam-to-column connections is through using gusset plates and bolts (Fig. 1). This type of connection consists of a gusset plate, sections of column and beam, and bolts.

Research focuses on investigating cold-formed structures [4-10] but there is a lack of connection-specific investigation. One of the possibilities on how to improve the accuracy of steel framework analysis could be through evaluations of the actual behaviour of joints [11-16]. For these purposes, the semi-rigid joint concept was introduced. This concept was developed mostly for hot-rolled sections and lacks application regulations for cold-formed sections. The most relevant influence on joint characteristics is produced by bending moments. In these cases, the behaviour of a semi-rigid joint is described by the moment–rotation  $M-\varphi$  curve of the joint. This concept has been adopted by most researchers and is consistent with design code EC3 [17].

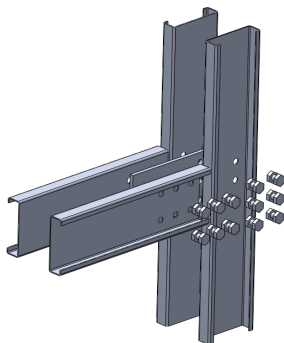


Fig. 1. Exploratory view of a bolted gusset-plate connection

In recent years, research on thin walled sections has focused on beam-to-column connections with gusset plates. The majority of these investigations were carried out on T-form or trapeze-form

gusset plate connections. Yu et al. [18] examined beam-to-column connections by executing sub-frame tests with different configurations of the gusset plate in plane. The influence of gusset plate thickness, chamfer presence, and the distance between bolts was investigated as pertaining to the strength and stiffness of the connections. The authors concluded that the geometry of a gusset plate has a huge impact on the behaviour of the connection. In the same article, a semi-empirical design method for calculating rotation stiffness of gusset plate connections was presented. In Bucmys and Sauciūvenas's paper [19] simulation data of the behaviour of beam to-column connections with T-form gusset plates has been presented. The authors examined the behaviour of gusset plate connections and took into account a variety of thicknesses and the geometrical structure of the gusset plate. Fang et al. [20] investigated the influence of initial imperfections and material strain hardening on the buckling behaviour of trapeze-form gusset plate connections. In the article the authors presented a method of calculating the strength of the connection out of plane buckling. Bucmys and Daniunas [21] proposed an investigation of the connection as the sum of three springs (Fig. 2): beam bolt group, column bolt group, and gusset plate. An analytical model of beam and column bolt groups and a technique of T-form gusset plate stiffness calculation were presented. All the authors of the paper reviewed agreed that the behaviour of bolted gusset plate connections is semi-rigid.

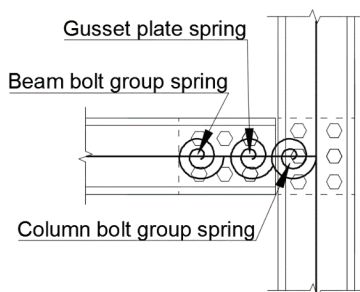


Fig. 2. The three-spring model

The paper's review revealed a lack of universal and accurate methods to calculate strength and stiffness of rectangular gusset plates. The goal of this paper is to present a method to evaluate rectangular gusset plates in terms of both strength and stiffness, and, moreover, to compare these results with laboratory testing and numerical simulation data.

## 2. ANALYTICAL MODEL OF GUSSET PLATE STRENGTH AND STIFFNESS CALCULATION

### 2.1. STRENGTH OF THE GUSSET PLATE

The moment resistance of a rectangular gusset plate was calculated assuming that the plate deforms only in plane. The design moment resistance of a rectangular gusset plate could be calculated according to the well-known formula:

$$(2.1) \quad M_{gp,Rd} = f_y \cdot W_{gp,pl}$$

where:

$f_y$  – yield strength of steel,  $W_{gp,pl}$  – plastic section modulus of section A-B or C-D weakened by bolts (fig. 3, 4)

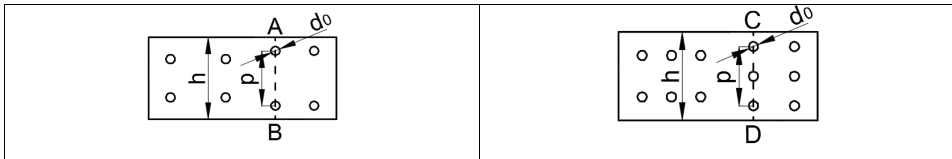


Fig. 3. A-B failure section

Fig. 4. C-D failure section

Plastic section modulus with two bolts in a column (2.2) and three bolts in a column (2.3) could be calculated:

$$(2.2) \quad W_{gp,pl} = \frac{t \cdot h^2}{4} - t \cdot d_0 \cdot p$$

$$(2.3) \quad W_{gp,pl} = \frac{t \cdot h^2}{4} - t \cdot d_0 \cdot p - \frac{t \cdot d_0^2}{4}$$

where:

$t$  – gusset plate thickness,  $h$  – height of gusset plate section,  $d_0$  – bolt hole diameter,  $p$  – distance between bolt holes

## 2.2. STIFFNESS OF THE GUSSET PLATE

The method of stiffness calculation presented in this chapter could be easily adapted to the three-spring mechanical model described in Bucmys and Daniunas previous [21] paper. The rotation of the rectangular gusset plate was investigated as the sum of deformations occurring at the bending moment and shear forces transmitted from the beam bolt group (Fig. 5). As a result, rectangular gusset plate rotation  $\varphi$  could be separated into  $\varphi_1$  and  $\varphi_2$  in result from the bending moment and shear force, respectively. In this paper, the initial stiffness of a gusset plate was calculated according to the formula:

$$(2.4) \quad S_{gp,ini} = \frac{M_{j,Ed}}{\varphi} = \frac{M_{j,Ed}}{\varphi_1 + \varphi_2} = \frac{M_{j,Ed}}{\frac{M_{1,Ed}L_a}{EI} + \frac{VL_a^2}{2EI}} = \frac{M_{j,Ed}}{\frac{2M_{1,Ed}L_a + VL_a^2}{2EI}}$$

where:

$L_a$  – distance from the rotation centre of the beam bolt group to the nearest row of bolts of the column bolt group,  $I$  – second moment of section A-B or C-D area (Fig. 3,4),  $V$  – shear force,  $E$  – Young modulus of steel,  $M_{1,Ed}$  – bending moment in the centre of the beam bolt group,  $M_{j,Ed}$  – bending moment in the centre of the column bolt group

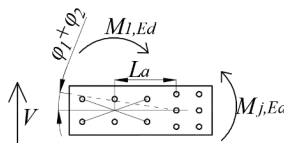


Fig. 5. The scheme for the rotation calculation of the gusset plate

The stiffness of a rectangular gusset plate could be calculated according a formula adapted from EC3:

$$(2.5) \quad S_{gp} = \frac{S_{gp,ini}}{\mu}$$

Stiffness coefficient  $\mu$  could be calculated according to EC3 design rules:

$$(2.6) \quad \left\{ \begin{array}{l} \text{if } M_{j,Ed} \leq 2/3 \cdot M_{j,Rd}, \text{ then } \mu = 1 \\ \text{if } 2/3 \cdot M_{j,Rd} < M_{j,Ed} \leq M_{j,Rd}, \text{ then } \mu = (1,5 \cdot M_{j,Ed} / M_{j,Rd})^{\psi} \end{array} \right.$$

where:

$\psi$  – for bolted connections 2,7,  $M_{j,Ed}$  – bending moment in the connection,  $M_{j,Rd}$  – The design moment resistance of the gusset plate.

### 3. EXPERIMENTAL TEST

Gusset plate-bolted beam-to-column connections were tested in order to investigate the behaviours of rectangular gusset plates. Test specimens consisted of beams and columns made out of cold-formed back-to-back lipped C-sections, rectangular gusset plates, and bolts. Two specimens were tested in the laboratory (Fig. 6, 7). Lateral supports were added to the beam, column, and joint, to prevent structure lateral displacement. Pinned support was added to the top of the column and roller support was added to its bottom column. The load was applied through a pinned connection to the end of the beam by a hydraulic jack. The deflection of the rectangular gusset plate was measured by a transducer through which the fastener was welded to the gusset plate. In this case, the transducer could rotate together with the column and measure only rectangular gusset plate deflection.

The specimens differed in thickness of the rectangular gusset plate and in distance between the bolts of the beam bolt group. Specimens M12C15025I10 and M12C15025I8 were fitted with 10 mm and 8 mm thick gusset plates (Fig. 8, 9), respectively. Rectangular gusset plates and cold-formed C-sections were made of S355 and S350GD+Z275 steel grade, respectively. Both specimens were connected using M12 bolts of 8.8 class. The diameter of the bolt holes was 13 mm. The beam and column of both specimens were made out of double back-to-back lipped C-sections. The width of the C-profile web, flange, and outstanding element was 150 mm, 40 mm and 22 mm, respectively. The thickness of the C-profile was 2.5 mm.

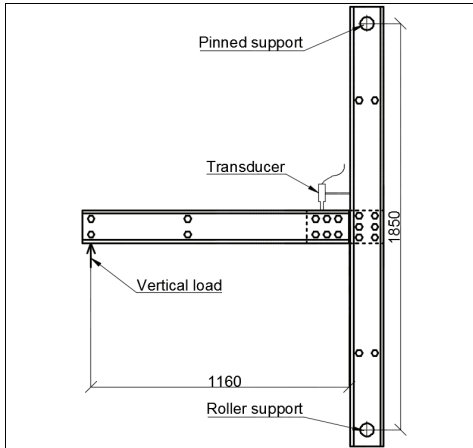


Fig. 6. Set of the experiment

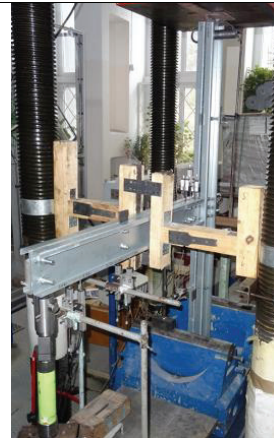


Fig. 7. Test specimen

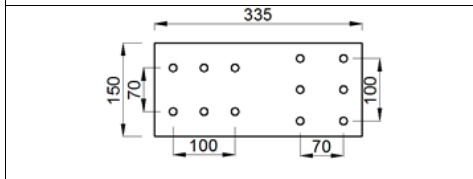


Fig. 8. Gusset plate of specimen M12C15025I10

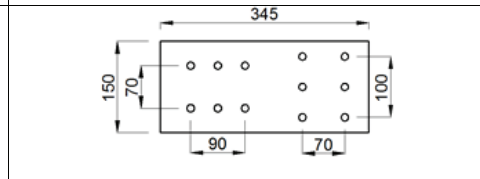


Fig. 9. Gusset plate of specimen M12C15025I8

Experimental bending capacity of specimens M12C15025I10 and M12C15025I8 was 17.39  $kNm$  and 14.74  $kNm$ , respectively. The failure mode of both specimens was the same: bolts in shear. After the demolition of the specimens it could be seen that bearing around bolt holes occurred, and the holes become oval in shape.

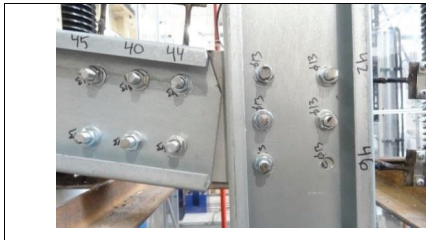


Fig. 10. Failure mode of specimen M12C15025I10



Fig. 11. Failure mode of specimen M12C15025I8

After tests of beam-to-column connection material properties, yield and ultimate strength were examined by executing tests of coupons. The following values have been obtained for C-

sections  $f_y = 380\text{MPa}$   $f_u = 484\text{MPa}$ , and for gusset plate  $f_y = 360\text{MPa}$   $f_u = 540\text{MPa}$ , respectively.

#### 4. NUMERICAL SIMULATION

Numerical simulation was performed using the ANSYS Workbench 14.0 finite element software, taking into account that this paper focuses on rectangular gusset plate behaviour only, gusset plates and column bolt groups were modelled.

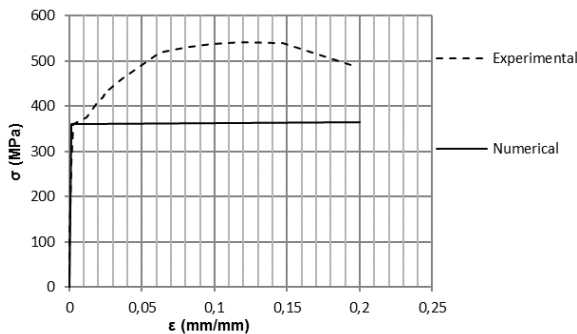


Fig. 12. Experimental and numerical stress - strain relationship

Steel was defined as an elastic plastic material with material properties taken from the coupon tests written about in the previous chapter (Fig. 12). The stress-strain relationship of a rectangular gusset plate was modelled according to EC3 [22] recommendations, whereby the elastic plastic part of the curve is recommended to be modelled as a horizontal or close-to-horizontal line. According to EC3 recommendations, this interpretation of the stress-strain relationship could be used for ultimate limit state criteria.



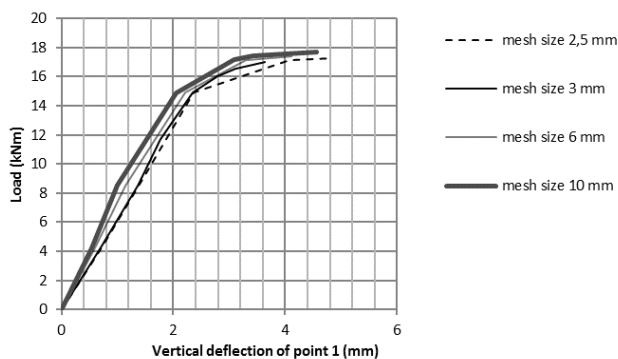


Fig. 13. Load–deflection curve

A mesh convergence study was executed to choose optimal mesh density of the numerical model. A rectangular gusset plate with 2,5 mm, 3 mm, 6 mm, and 10 mm double-layer mesh was forged. Load–deflection curves (Fig. 13) show that the vertical deflection of point 1 (Fig. 14) increases as the mesh density decreases. But it is also seen that the vertical deflection increase slows when mesh density as at 3 mm. As a result, mesh density of the rectangular gusset plate and bolts (Fig. 14) was chosen to be 3 mm. Three-dimensional solid elements SOLID186 and SOLID187 were used for modelling. This element is suitable for geometric and material nonlinear behaviour analysis.

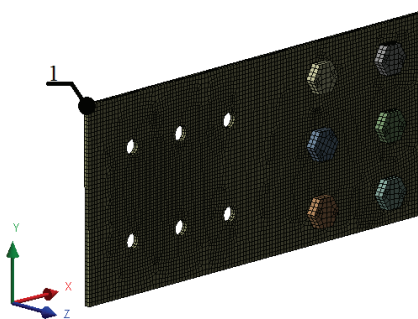


Fig. 14. Finite element model

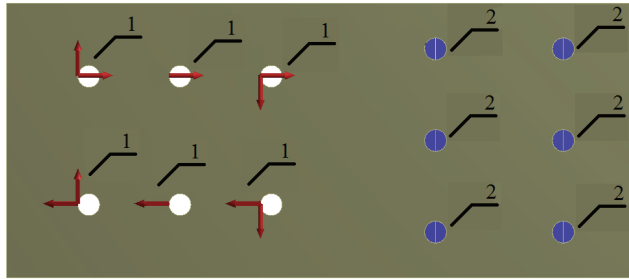


Fig. 15. 1- Load direction and 2- fixed connections of bolts

Equivalent Stress  
Type: Equivalent (von-Mises) Stress  
Unit: MPa

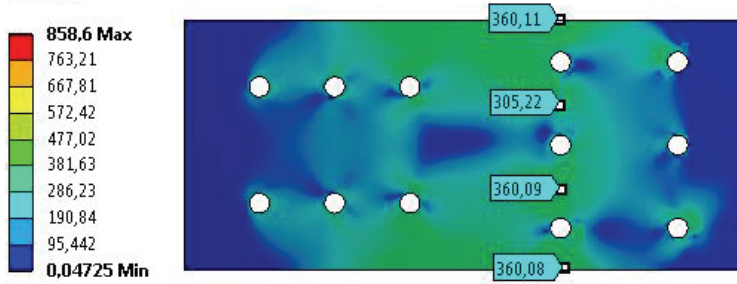


Fig. 16. Von-Mises stress distribution of specimen M12C15025110

Equivalent Stress  
Type: Equivalent (von-Mises) Stress  
Unit: MPa

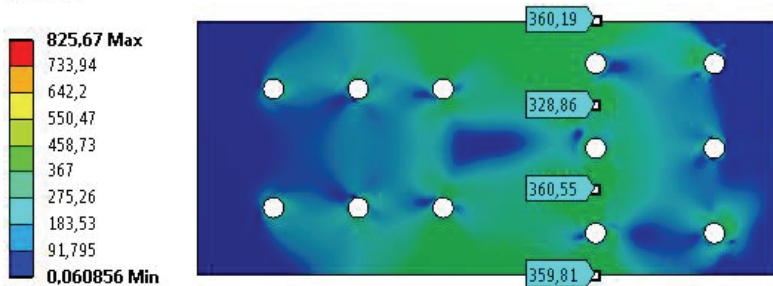


Fig. 17. Von-Mises stress distribution of specimen M12C1502518

Geometrical and material nonlinear analysis was performed; this type of analysis was chosen because of contact and it was expected that the rectangular gusset plate would yield. To perform this type of analysis, nonlinear material behaviour was modelled as described before, and a load was added using approximately ten steps. Symmetrical conditions were used parallel to the  $x-y$  plane (Fig. 14), meaning that only half of the rectangular gusset plate and bolts were modelled, which allows for a double decrease in the amount of finite elements.

Rough contact conditions were used between the rectangular gusset plate and the column bolt group bolts; frictional contact where no sliding occurs. This case corresponds to an infinite friction coefficient and ignores material property. The beam bolt group was not modelled, but loading was added as horizontal and vertical forces to the beam bolt holes (Fig. 15). These forces simulate a bending moment and shear force which is transferred from the beam bolt group to the rectangular gusset plate. Finally, bolts of the column bolt group were connected using fixed connections.

As expected, the failure mode of both specimens was flexural failure of the gusset plate. As it is depicted in Fig. 16 and Fig. 17, stress values where the bending moment is the highest in the rectangular gusset plate cross-section reached yield strength values. Specimens M12C15025I10 and M12C15025I8 failed at 23,28  $kNm$  and 16,63  $kNm$ , respectively.

Type: Directional Deformation(Y Axis)  
Unit: mm

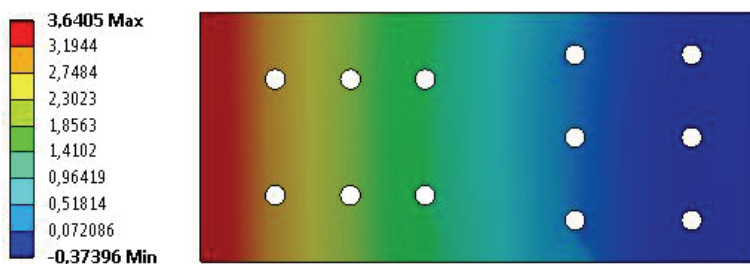


Fig. 18. Deflections of specimen M12C15025I10

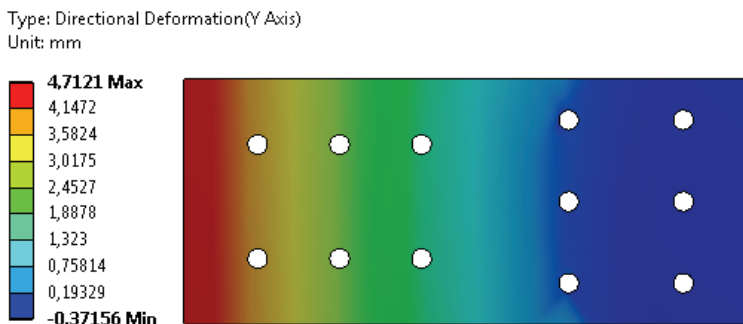


Fig. 19. Deflections of specimen M12C15025I8

According to the modelling technique previously described, four more specimens were modelled through changing the thickness of the rectangular gusset plate. The geometry of a rectangular gusset plate was taken as well as that of specimens M12C15025I8 and M12C15025I10 with 6 mm and 12 mm gusset plate thickness, M12C15025I8-6, M12C15025I8-12, M12C15025I10-6, and M12C15025I10-12, respectively. The deflections of specimens M12C15025I10 and M12C15025I8 is depicted in Fig. 18 and Fig. 19.

## 5. RESULTS

The  $M-\varphi$  relationship of specimens using the analytical method, experimental testing and numerical simulation of all specimens is depicted in Figs. 20-23. Bending capacity and initial stiffness of a rectangular gusset plate is presented in Table 1. Bending capacity of a rectangular gusset plate calculated using the presented analytical model compared with numerical solution results of specimens M12C15025I10, M12C15025I10-6, and M12C15025I10-12 was lower by 7 – 11% and of specimens M12C15025I8, M12C15025I8-6, and M12C15025I8-12 was higher by 8 – 10%. Analytical bending capacity of specimens M12C15025I10 and M12C15025I8 was lower by 8% and 9%, respectively. Initial stiffness of the connections obtained according to the presented analytical model comparison of specimens M12C15025I10 and M12C15025I8 was higher by 9% and lower by 6% than the experimental, respectively. Initial stiffness of specimens M12C15025I10 and M12C15025I10-12 calculated using the presented analytical model was lower compared with numerical simulation results by 6% and 9%, respectively. All remaining specimens showed initial stiffness higher by 5 – 12% when calculated using the presented analytical model (over the

numerical simulation). All the results collected demonstrate that the proposed analytical model for calculating both strength and stiffness of rectangular gusset plates satisfactorily correlate with experimental testing and numerical simulation results. This shows that the presented analytical model could be used for calculating rectangular gusset plate component properties and could be integrated to aid in evaluating joint strength and stiffness using the component method.

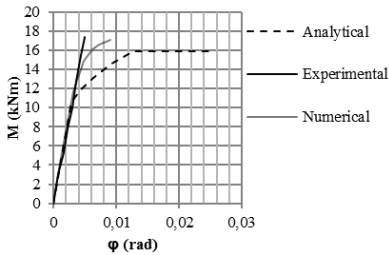


Fig. 20.  $M$ - $\varphi$  relationship of specimen M12C15025I10

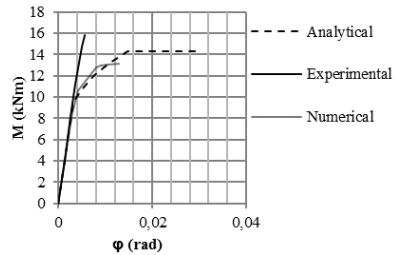


Fig. 21.  $M$ - $\varphi$  relationship of specimen M12C15025I8

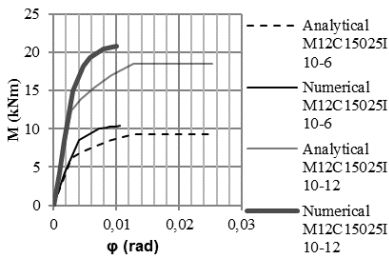


Fig. 22.  $M$ - $\varphi$  relationship of specimens M12C15025I10-6 and M12C15025I10-12

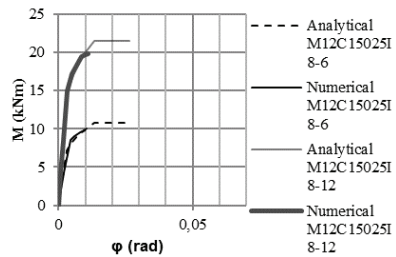


Fig. 23.  $M$ - $\varphi$  relationship of specimens M12C15025I8-6 and M12C15025I8-12

Table 1. Results of the analytical model, FEM and experimental investigation

Specimen	$M_{Rd,analytical}$ (kNm)	$M_{Rd,FEM}$ (kNm)	$S_{ini,analytical}$ (MNm/rad)	$S_{ini,exp}$ (MNm/rad)	$S_{ini,BEM}$ (MNm/rad)
M12C15025I10	15,86	17,03	3,75	3,43	3,78
M12C15025I8	14,30	13,12	2,91	3,11	2,76
M12C15025I10-6	9,25	10,35	2,19	-	2,12
M12C15025I10-12	18,50	20,79	4,38	-	4,79
M12C15025I8-6	10,72	9,75	2,44	-	2,25
M12C15025I8-12	21,45	19,83	4,87	-	4,36

## 6. CONCLUSIONS

An analytical model of the component method for calculating strength and stiffness of cold-formed steel beam-to-column gusset plate joints is presented herein. The strength and stiffness investigation of rectangular gusset plates in cold-formed I-type steel connections presented in this paper allows us to make the following conclusions:

- The proposed analytical model extends the existing component method and allows for the evaluation of the strength and stiffness properties of cold-formed I-type steel connections of rectangular gusset plate components.
- Experimental tests and numerical simulations both show that the rectangular shape of a gusset plate has an impact on joint stiffness.
- The presented technique of calculating rectangular gusset plate stiffness and evaluating the  $M-\varphi$  curves could be fully integrated with the component method rules presented in part 1993-1-8 of the Eurocode.
- The calculation results of the proposed analytical model were compared against 2 laboratory tests and 6 numerical simulation models. When looking at both the proposed analytical model and the numerical simulation results, bending capacity and initial stiffness differed up to 11% and up to 12%, respectively. Final results showed that the presented analytical model shows satisfactory agreement and is applicable in such instances of component strength and stiffness evaluation.

## REFERENCES

1. Yang J., Liu Q., "Sleeve connections of cold-formed steel sigma purlins", *Engineering structures*, 43: 245 – 258, 2012.
2. Dawe J. L., Liu, Yi, Li, J. Y., "Strength and behaviour of cold-formed steel offset trusses", *Journal of constructional steel research*, 66: 556-565, 2010.
3. Pedreschi R. F., Sinha B. P., "An experimental study of cold formed steel trusses using mechanical clinching", *Construction and Building Materials*, 22: 921–931, 2008.
4. Piotrowski R., Szychowski A., "Lateral-Torsional Buckling of Beams Elastically Restrained Against Warping at Supports", *Archives of Civil Engineering*, 61: 155–174, 2015.
5. W.-W. Yu, R. A. LaBoube, "Cold-Formed Steel Design". Fourth ed. United States of America: John Wiley & Sons, 2010.
6. Rzeszut K., Polus Ł., "Numerical Analysis of Thin-Walled Purlins Restrained by Sheeting in Elevated Temperature Conditions", *Archives of Civil Engineering*, 61: 35–46, 2015.
7. Szychowski A., "Buckling Of The Stiffened Flange Of The Thin-Walled Member At Longitudinal Stress Variation", *Archives of Civil Engineering*, 61: 149–168, 2015.
8. Bitarafan M., Zolfani S. H., Arefi S. L., Zavadskas E. K., "Evaluating the construction methods of cold-formed steel structures in reconstructing the areas damaged in natural crises, using the methods AHP and COPRAS-G", *Archives of civil and mechanical engineering*, 12: 360-367, 2012.
9. Lim, J. B. P., Nethercot, D. A. "Stiffness prediction for bolted moment-connections between cold-formed steel members", *Journal of Constructional Steel Research*, 60: 85–107, 2004.
10. Sabbagh, A. B., Petkovski, M., Pilakoutas, K., Mirghaderi, R., "Cyclic behaviour of bolted cold-formed steel moment connections: FE modelling including slip", *Journal of Constructional Steel Research*, 80: 100–108, 2013.
11. Bródka J., "Design Of Hollow Section Overlap Joints With Reinforcing Rib Plate. Joint Resistance", *Archives of Civil Engineering*, 61: 3–16, 2015.
12. Bródka J., Broniewicz M., "Design Of Hollow Section Overlap Joints With The Reinforcing Rib Plate. Welded Connection Resistance", *Archives of Civil Engineering*, 61: 17–44, 2015.
13. Gečys, T.; Daniūnas, A.; Bader T. K.; Wagner L.; Eberhardsteiner J., "3D finite element analysis and experimental investigations of a new type of timber beam-to-beam connection", *Engineering structures*, 86: 134-145, 2015.
14. Daniūnas A.; Urbonas, K., "Analysis of the steel frames with the semi-rigid beam-to-beam and beam-to-column knee joints under bending and axial forces", *Engineering Structures*. 30 (11): 3114-3118, 2008.
15. Kala, Z., "Reliability analysis of the lateral torsional buckling resistance and the ultimate limit state of steel beams with random imperfections", *Journal of Civil Engineering and Management* 21(7): 902–911, 2015.
16. Kala, Z., "Global sensitivity analysis in stability problems of steel frame structures", *Journal of Civil Engineering and Management* 22(3): 417–424, 2016.
17. EN 1993-1-8: 2005: Eurocode 3 - Design of steel structures - Part 1-8: Design of joints. Comité Européen de Normalisation, Brussels.
18. Yu W. K., Chung K. F., Wong M. F., "Analysis of bolted moment connections in cold-formed steel beam-column sub-frames", *Journal of constructional steel research*, 61: 1332-1352, 2005.
19. Bucmys, Z., Sauciūvenas, G., "The behaviour of cold formed steel structure connections", *Engineering structures and technologies*, 5: 113-122, 2013.
20. Fang C., Yam M. C. H., Zhou X., Zhang Y. "Post-buckling resistance of gusset plate connections: Behaviour, strength, and design considerations", *Engineering structures*, 99: 9-27, 2015.
21. Bucmys, Z., Daniūnas, A., "Analytical and experimental investigation of cold-formed steel beam-to-column bolted gusset-plate joints", *Journal of Civil Engineering and Management*, 21: 1061-1069, 2015.
22. EN 1993-1-5:2006: Eurocode 3 - Design of steel structures - Part 1-5: Plated structural elements. Comité Européen de Normalisation, Brussels.

*Received 20.01.2017*

*Revised 28.03.2017*

**LIST OF FIGURES AND TABLES:**

Fig. 1. Exploratory view of a bolted gusset-plate connection

Rys. 1. Widok rozstrzelony śrubowego połączenia blachy węzłowej

Fig. 2. The three-spring model

Rys. 2. Trzyczęściowy model

Fig. 3. A-B failure section

Rys. 3. Obszar awarii A-B

Fig. 4. C-D failure section

Rys. 4. Obszar awarii C-D

Fig. 5. The scheme for the rotation calculation of the gusset plate

Rys. 5. Schemat obliczania obrotu blachy węzłowej

Fig. 6. Set of the experiment

Rys. 6. Zestaw eksperymentów

Fig. 7. Test specimen

Rys. 7. Próbkę do badania

Fig. 8. Gusset plate of specimen M12C15025I10

Rys. 8. Blacha węzłowa próbki M12C15025I10

Fig. 9. Gusset plate of specimen M12C15025I8

Rys. 9. Blacha węzłowa próbki M12C15025I8

Fig. 10. Failure mode of specimen M12C15025I10

Rys. 10. Tryb awaryjny próbki M12C15025I10

Fig. 11. Failure mode of specimen M12C15025I8

Rys. 11. Tryb awaryjny próbki M12C15025I8

Fig. 12. Experimental and numerical stress - strain relationship

Rys. 12. Naprężenie doświadczalne i liczbowe – związek naprężeń

Fig. 13. Load-deflection curve

Rys. 13. Obciążenie – krzywa odkształcenia

Fig. 14. Finite element model

Rys. 14. Model elementów skończonych

Fig. 15. 1- Load direction and 2- fixed connections of bolts

Rys. 15. 1- Kierunek obciążenia i 2 – stałe połączenia śrub

Fig. 16. Von-Mises stress distribution of specimen M12C15025I10

Rys. 16. Rozkład naprężeń Von-Misesa w próbce M12C15025I10

Fig. 17. Von-Mises stress distribution of specimen M12C15025I8

Rys. 17. Rozkład naprężeń Von Misesa w próbce M12C15025I8



Fig. 18. Deflections of specimen M12C15025I8

Rys. 18. Odkształcenia próbki M12C15025I8

Fig. 19. Deflections of specimen M12C15025I10

Rys. 19. Odkształcenia próbki M12C15025I10

Fig. 20.  $M-\varphi$  relationship of specimen M12C15025I10

Rys. 20. Związek  $M-\varphi$  próbki M12C15025I10

Fig. 21.  $M-\varphi$  relationship of specimen M12C15025I8

Rys. 21. Związek  $M-\varphi$  próbki M12C15025I8

Fig. 22.  $M-\varphi$  relationship of specimens M12C15025I10-6 and M12C15025I10-12

Rys. 22. Związek  $M-\varphi$  próbek M12C15025I10-6 i M12C15025I10-12

Fig. 23.  $M-\varphi$  relationship of specimens M12C15025I8-6 and M12C15025I8-12

Rys. 23. Związek  $M-\varphi$  próbek M12C15025I8-6 i M12C15025I8-12

Tab. 1. Results of the analytical model, FEM and experimental investigation

Tab. 1. Wyniki modelu analitycznego, FEM i badania eksperymentalnego

## ZACHOWANIE PROSTOKĄTNEJ BLACHY WĘZŁOWEJ W POŁĄCZENIACH STALOWCH TYPU I, FORMOWANYCH NA ZIMNO

*Słowa kluczowe:* połączenia stalowe formowane na zimno, połączenia półsztywne, wytrzymałość, sztywność

### STRESZCZENIE:

Cienkościenne przekroje formowane na zimno są szeroko stosowane jako konstrukcje nośne. W większości przypadków, cienkościenne przekroje pełnią funkcję płatew, kratownic stalowych oraz lekkich ram portalowych. Połączenia takich konstrukcji powinny być proste, szybkie i łatwe w instalacji. Jednym z najprostszych sposobów połączenia belki nośnej z kolumną jest zastosowanie blach węzłowych i śrub. Ten rodzaj połączenia składa się z blachy węzłowej, przekrojów kolumny i belki nośnej oraz śrub. Przegląd prac wykazał brak uniwersalnych i dokładnych metod obliczania wytrzymałości i sztywności prostokątnych blach węzłowych. Celem niniejszej pracy jest przedstawienie metody oceny prostokątnej blachy węzłowej, zarówno pod względem wytrzymałości jak i sztywności. Ponadto, skupia się ona na porównaniu tych wyników z danymi dotyczącymi badania laboratoryjnego i danych numerycznej symulacji. Niniejsza praca zawiera metodę oceny wytrzymałości i sztywności prostokątnej blachy węzłowej. Zachowanie zostało zbadane przy założeniu, że blacha ulega deformacji wyłącznie w płaszczyźnie. Obrót prostokątnej blachy węzłowej został zbadany jako suma deformacji będących wynikiem sił zginania i ścinania, które są przenoszone z grupy śrub. Preparaty EC3 zostały dostosowane do przedstawionej metody obliczania sztywności.

Zbadano śrubowe połączenie belki nośnej z kolumną w prostokątnej blasze węzłowej, w celu sprawdzenia zachowania prostokątnej blachy węzłowej. Próbkę do badania składały się z belek nośnych i kolumn wykonanych z równoległych przekrojów typu C formowanych na zimno, prostokątnej blachy węzłowej oraz śrub. W laboratorium przeprowadzono badanie dwóch próbek. Odchylenie prostokątnej blachy węzłowej zostało zmierzone za pomocą przetwornika, który za pomocą łącznika został przyspawany do prostokątnej blachy węzłowej. W tym przypadku przetwornik mógłby obracać się wraz z kolumną i dokonywać pomiarów wyłącznie odchylenia prostokątnej blachy węzłowej. Próbki różniły się pod względem grubości prostokątnej blachy węzłowej oraz odległości pomiędzy śrubami z grupy. Próbki M12C15025I10 i M12C15025I8 obejmowały odpowiednio prostokątne blachy węzłowe o grubości 10 mm i 8 mm. Doświadczalna zdolność do gięcia próbek M12C15025I10 i M12C15025I8 obejmowała odpowiednio 17,39 kNm i 14,74 kNm. Tryb awaryjny obu próbek był taki sam: śruby w ścinaniu. Po rozłożeniu próbek na czynniki pierwsze, zaobserwowano pojawienie się łóżysek przy otworach śrubowych. W rezultacie otwory śrubowe przyjęły kształt owalny.

Symulacja numeryczna została przeprowadzona przy użyciu oprogramowania elementów skończonych ANSYS Workbench. Uwzględniła ona fakt, iż niniejsza praca skupia się na zachowaniu prostokątnej blachy węzłowej. Wyłącznie grupa śrubowa blachy węzłowej i kolumny została poddana modelowaniu. Do modelowania użyto trójwymiarowych elementów stałych SOLID186 i SOLID187. Zgodnie z oczekiwaniami, tryb awaryjny obu próbek był wadą zginania prostokątnej blachy węzłowej. Próbki M12C15025I10 i M12C15025I8 wyniosły odpowiednio 23,28 kNm i 16,63 kNm. Zgodnie z opisaną techniką modelowania, modelowanie obejmowało 4 kolejne próbki poprzez zmianę grubości prostokątnej blachy węzłowej. Zastosowano geometrię prostokątnej blachy węzłowej, jak również próbek M12C15025I8 i M12C15025I10 z grubością blachy węzłowej wynoszącą 6 mm i 13 mm, jak również odpowiednio M12C15025I8-6, M12C15025I8-12, M12C15025I10-6 oraz M12C15025I10-12.

Niniejsza praca opisuje stosunek  $M-\varphi$  próbek z wykorzystaniem metody analitycznej, badania doświadczalnego i symulacji numerycznej wszystkich próbek. Zdolność gięcia prostokątnej blachy węzłowej, obliczana przy użyciu przedstawionego modelu analitycznego, w porównaniu z wynikami obliczeń numerycznych próbek M12C15025I10, M12C15025I10-6 i M12C15025I10-12, była mniejsza o 7-11%, a w przypadku próbek M12C15025I8, M12C15025I8-6 i M12C15025I8-12 – większa o 8-10%. Analityczna zdolność gięcia próbek M12C15025I10 i M12C15025I8 była mniejsza o 8% i 9%, odpowiednio. Początkowa sztywność połączenia uzyskanego zgodnie z przedstawionym modelem analitycznym porównania próbek M12C15025I10 i M12C15025I8 była większa o 9% i mniejsza o 6% od eksperymentalnej. Początkowa sztywność próbek M12C15025I10 i M12C15025I10-12, obliczona za pomocą przedstawionego modelu analitycznego, była mniejsza w porównaniu z wynikami symulacji numerycznej, tj. odpowiednio 6% i 9%. Wszystkie pozostałe próbki wykazały większą początkową sztywność (o 5%-12%), obliczoną przy użyciu przedstawionego modelu analitycznego. Wszystkie wyniki wykazują, że zaproponowany model analityczny dla prostokątnej blachy węzłowej, zarówno w odniesieniu do obliczeń wytrzymałości jak i sztywności, w sposób zadowalający koreluje z wynikami badania eksperymentalnego i symulacji numerycznej. Niniejsza praca pokazuje, że przedstawiony model analityczny może być stosowany podczas obliczeń właściwości elementów blachy węzłowej i może być zintegrowany ze wspólną oceną wytrzymałości i sztywności przy użyciu metody składowych.

Badanie prostokątnej blachy węzłowej w stalowych połączeniach typu I, formowanych na zimno, pozwala nam wyciągnąć następujące wnioski:

- Proponowany model analityczny stanowi rozszerzenie metody składowych i pozwala na dokonanie oceny właściwości wytrzymałości i sztywności elementów prostopadłej blachy węzłowej w zakresie stalowych połączeń typu I, formowanych na zimno.
- Badania eksperymentalne i symulacja numeryczna wykazały, że prostokątna blacha węzłowa ma wpływ na sztywność złączy.
- Przedstawiona technika obliczania sztywności prostopadłej blachy węzłowej i oceny krzywych  $M-\varphi$  może być w pełni zintegrowana z zasadami dotyczącymi metody składowych, opisanymi w Eurokodzie, część 1999-1-8.
- Wyniki obliczeń proponowanego modelu analitycznego zostały porównane z 2 badaniami laboratoryjnymi oraz 6 modelami symulacji numerycznej.

Podczas dokonywania porównania zarówno wyników proponowanego modelu analitycznego i symulacji numerycznej, zdolność gięcia i początkowa sztywność różniły się odpowiednio o 11% i 12%. Wyniki wykazały, że przedstawiony model analityczny jest zadowalający i odpowiedni do oceny takiej wytrzymałości i sztywności.

